Heat Transfer on the Bottom of a Vessel Agitated by the Impeller Embedded in the Draft Tube

Marcela Věříšová[1*]

[1] *CTU in Prague, Faculty of Mechanical Engineering, Department of Process Engineering, Technická 4, 166 07 Praha 6, Czech Republic*

Abstrakt

The paper is concerned with measurement of local heat transfer on a flat bottom of an agitated vessel using the electro-diffusion method. The experiments were performed in a cylindrical vessel with the flat bottom and agitated by an axial high-speed impeller, which was embedded in the draft tube. This draft tube provided a clearly defined flow imitating a submerged confined jet impinging the vessel bottom. The results are presented in the dependency of the Nusselt number on the non-dimensional radial distance from the stagnation point. In addition, the similarity between classic impinging jet and rotating impinging jet is shown.

Keywords: heat transfer, electro-diffusion method, impinging jet

1. Introduction

The impingement jet is well known to give a high heat transfer coefficient near the stagnation region where the jet impinges on the target plate, therefore it is widely used as an effective technology in many branches of industries. The applications include cooling of heated components of turbine engines and of combustor walls, cooling of electronic equipment, processing of some metals and glass, deicing of aircraft systems, drying of textile, food products, films and papers. Impinging jet is provided high local heat and mass transfer coefficient also in mechanically agitated equipment.

For good description of the mixing system behavior is important to determine both hydraulic properties of the impinging jet and local and average values of heat transfer coefficient. Heat transfer rate in case of impinging jets are affected by various parameters like Reynolds number, jet-to-plate distances, radial distance from stagnation point, Prandtl number, target plate inclination, confinement of the jet, nozzle geometry, curvature of target plate, roughness of the target plate and turbulence intensity at the nozzle exit.[1]

The objective of this study was put on finding of similarities in the flow and heat transfer characteristic between results of a round impinging jet and results of experimental data obtained on an agitated vessel with an axial flow impeller embedded in the draft tube with four baffles. In the case with an axial impeller in a draft tube was provided a clearly defined flow imitating a submerged confined jet impinging the vessel bottom.

The flow field of the impinging jet is characterized as the combination of four regions, as illustrated in the left side of **Fig. 1**. The first is a free jet region which develops instantly at the nozzle exit (I). At a certain distance over the surface, the free jet is transformed into a stagnation flow region (II) where the vertical component of the velocity is reduced to zero, whereas the horizontal component increases from zero to maximum value at a certain distance from the stagnation point. Then, the transition region (III) follows and it is transformed into a wall jet (in the case of an unconfined geometry) which, like the free jet, is characterized by widening and deceleration. [1]

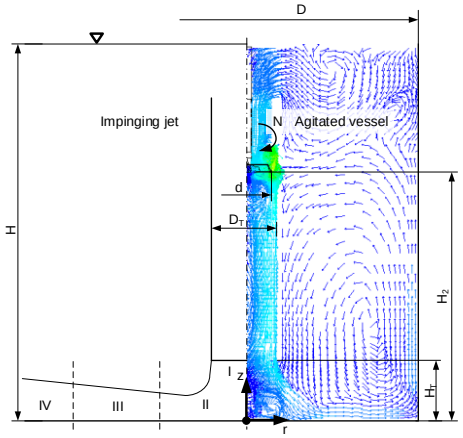

Fig. 1. Similarities between the impinging jet flow regions and flow patterns near walls and bottom in a vessel agitated by an axial high-speed impeller [1]

The flow of liquid directed by an axial impeller toward the bottom and the wall of a cylindrical vessel can be expressed as a sequence of impact and wall turbulent flows, (see **Fig. 2,** [2]). In the right side of **Fig. 1.** one can see flow patterns obtained from CFD near walls and bottom in a vessel agitated by an axial high-speed impeller embedded in draft tube. In this configuration both high axial pumping effect and circulation effects are reached. The impeller one can imagine as axial pump and a discharge from the draft tube is characterized as a submerged rotating impinging jet, in this case. It is possible to recognize certain similarity in the flow and heat transfer characteristics between round impinging jet and rotating impinging jet. The heat transfer at the vessel bottom differs from the classic impinging jet by the tangential velocity component generated by the rotating impeller. The axial

* Kontakt na autora: marcela.verisova@fs.cvut.cz

impeller forms a swirling axially symmetrical free stream (I), then it changes into so called impact jet (II) with a change in its direction, concurrent with a modification of its character. This jet changes its direction at the bottom and it is possible to consider the so called radial wall jet (III). The velocity profile of radial wall jet is affected by the shape of the profile in the preceding free jet and by the existence of the bottom solid wall. Then it changes into impact jet (IV), which is affected by the presence of a solid wall again, and after another smooth change of stream direction axial wall jet forms (V). The character of this stream is again affected by the presence of solid wall, or baffles and by the radial velocity profile.

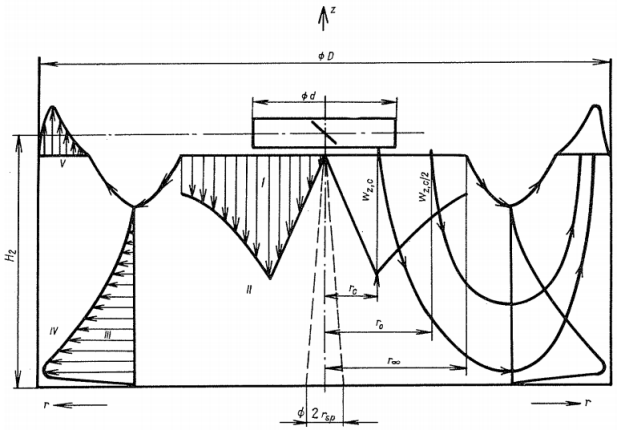

Fig. 2. Flow patterns in a vessel agitated by an axial impeller [2]

On the basis of these two type of flow pattern, can be supposed, that some similarities be founded.

Many researches on impinging jet in literature has been carried out experimentally, analytically and numerically. A large amount of data is available for single, rows and arrays of impinging jet with also correlations for heat and mass transfer.

For example Katti et al [4] performed an experimental investigation of the effect of jet to plate spacing and low Reynolds number on the local heat transfer distribution to normally impinging submerged circular air jet on a smooth and flat surface. They published correlation for average Nusselt number as a function of h/d and Reynolds numbers for $0.5 \leq h/d \leq 8$ and $500 \leq Re \leq 8000$.

$$\overline{Nu} = 0.11 Re^{0.69} \Pr^{0.33} \left(\frac{h}{d}\right)^{-0.4} \qquad (1)$$

Where h is nozzle place spacing and d is diameter of the nozzle exit.

Bovo [12] concerned with heat transfer in impinging jets using CFD. Stationary impinging jets with different nozzle-to-wall distances and Reynolds number were modelled. He determined Nusselt numbers and plotted them against the non-dimensional radial distance from the stagnation point.

2. Method

Local heat transfer coefficients were studied experimentally using the electro-diffusion method based on the measurement of the limiting diffusion current on a working electrode for equimollar the ferri/ferro-cyanide system in alkaline solution. In this method, the diffusion current measured is proportional to the mass transfer coefficient k_A. The electrolyte consisted from 20mol.m^{-3} potassium ferricyanide, 20mol.m^{-3} potassium ferrocyanide and 1.5% mass sodium hydroxide. The density of the solution was 1017kg.m^{-3} kinematic viscosity 8.893x10^{-7}m^2.s^{-1} and diffusivity 7.5x10^{-10} at 20°C. Properties of distilled water were used in place of other necessary properties. The number of electrons involved in the electrochemical reaction was equal to 1. Twelve small platinum electrodes of 0.5 mm diameter were positioned in the radial direction at the vessel bottom. Local heat transfer coefficients were calculated on the basis of the assumed analogy between mass and heat transfer process by the following formula[4]

$$\alpha = c_p \rho \left(\frac{Sc}{Pr}\right)^{2/3} k_A = c_p \rho \left(\frac{Sc}{Pr}\right)^{2/3} \frac{I}{zFc_A A}, \qquad (2)$$

where c_p is the specific heat capacity, ρ is the liquid density, Sc is the Sherwood number, Pr is the Prandtl number, k_A is the mass transfer coefficient, I is the limiting diffusion current, z is the number of electrons involved in the electrochemical reaction, F is the Faraday constant, c_A is molar concentration of the active component in electrolyte and A is surface of the working electrode.

Fig. 3 shows a schematic of the experimental apparatus. All experiments were performed in an agitated vessel and inner diameter D=390mm. The vessel without the baffles was made from PMMA and filled by electrolyte up to height H=430 mm. The vessel was equipped with flow-directing devices – draft tube. The draft tube was length L=300 mm and inner diameter D_T=70mm and was made from PMMA and situated H_T=70mm above the vessel bottom. Four baffles (l/d=1) were placed along the draft tube circumference by 90-degree. The axial six-blade impellers with pitched angle 30°, 45° and 60° and 61 mm in diameter, embedded in a draft tube, was placed in a cylindrical vessel with flat bottom.

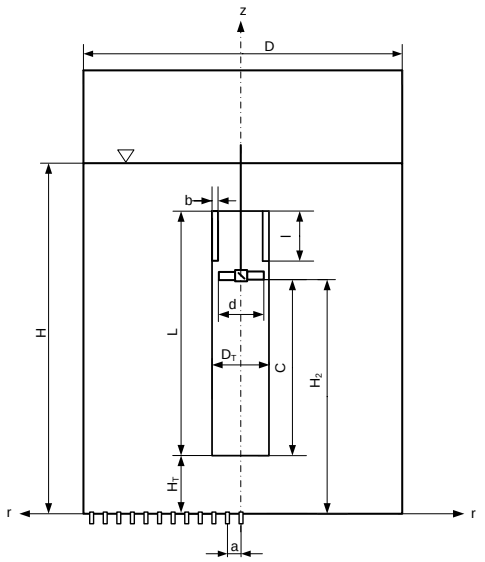

Fig. 3. Experimental setup

The flow intensity for mixing processes can be described by the modified Reynolds number defined as [6]

$$Re_M = \frac{Nd^2}{\nu}, \quad (3)$$

where N is the impeller rotation speed, d is impeller diameter and ν is kinematic viscosity.

The local heat transfer intensity is usually expressed in dimensionless form of Nusselt number as [7]

$$Nu = \frac{\alpha D_T}{\lambda}, \quad (4)$$

where α is the local heat transfer coefficient, D_T is draft tube diameter and λ is the thermal conductivity of fluid.

An axial flow impeller produces a swirling jet impinging the vessel bottom. The amount of liquid leaving the impeller zone in the axial direction can be characterized by the pumping capacity[8]

$$\dot{Q} = N_{QP} N d^3, \quad (5)$$

where N_{QP} is dimensionless axial pumping capacity of impeller, N is the impeller rotation speed, d is impeller diameter.

From the knowledge of pumping capacity one can calculate value of velocity

$$u = \frac{\dot{Q}}{\frac{\pi D_T^2}{4}}, \quad (6)$$

by means of which is Reynolds number re-count [9]

$$Re = \frac{uD_T}{\nu} \quad (7)$$

In **Fig. 4**. and **Fig. 5** are illustrated radial profiles of dimensionless axial and tangential velocity components.[10]

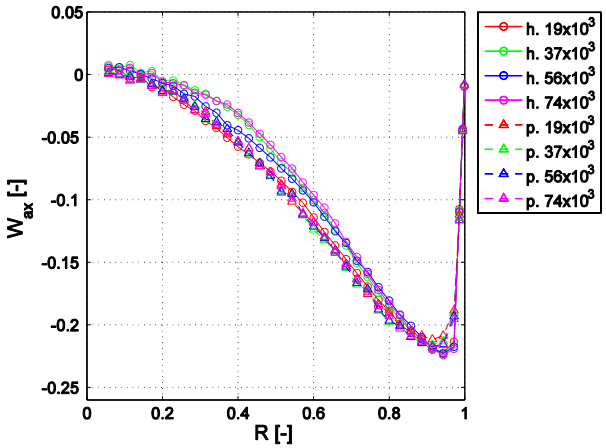

Fig. 4. Radial profile of dimensionless axial velocity in the exit of the draft tube [10]

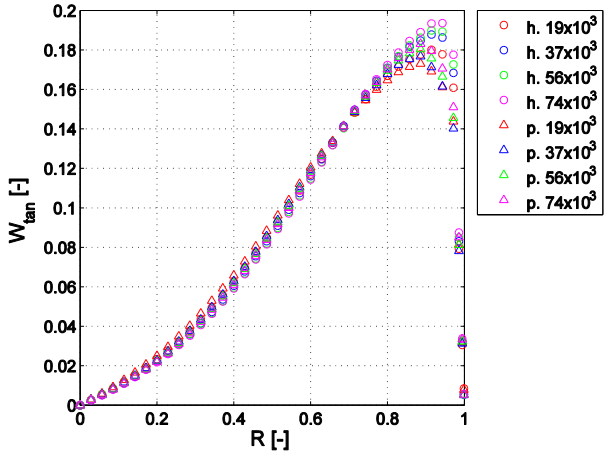

Fig. 5. Radial profile of dimensionless tangential velocity in the exit of the draft tube [10]

3. Results

In **Fig. 7.**, **Fig. 8. and Fig. 9**. dependence of the Nusselt number on the dimensionless radial coordinate positions of working electrodes are shown. The dimensionless coordinates were obtained as ratio of radial coordinate to draft tube diameter.

It can be seen, that there are three peak in these dependency. The first one is in the stagnation point, second one is occurred in vicinity $r/D_T=1$ and the third one is found in the vicinity of $r/D_T=1.75$.

There are many these dependencies in the literature. But it is only for configuration without confine by solid axial wall. And in these dependencies only one or two peaks are occurred.

The phenomenon of the second peak is not fully understood, but Bovo [12] presents three possible explanations of that.

The third peak is probably caused that fluid flow changes its direction due to presence solid vertical wall. In **Fig. 6**. dependence of the Nusselt number on the dimensionless radial coordinate positions of working electrodes for the impinging jet from nozzle are shown.

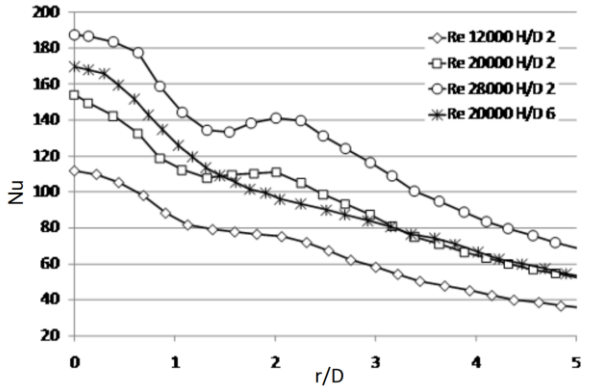

Fig. 6. Distribution of local Nusselt number at various H_D/D at different Reynolds number for impinging jet [12]

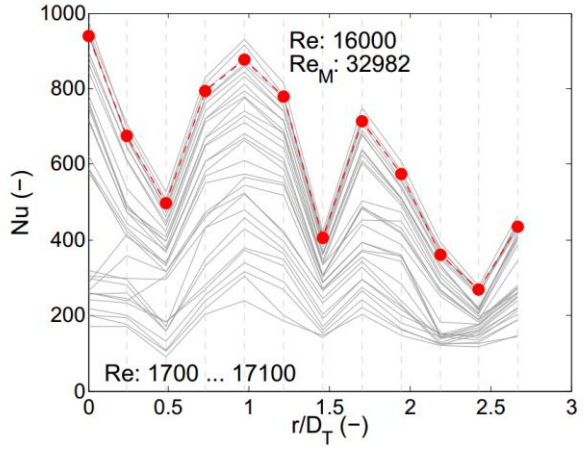

Fig. 7. Distribution of local Nusselt number at H_D/D_T=1at different Reynolds number for impeller with pitch angle 30°

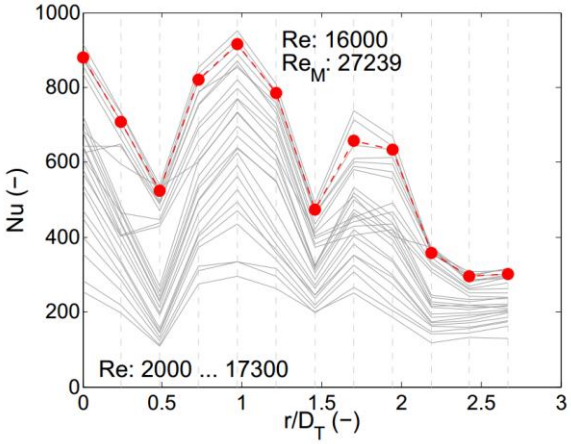

Fig. 8. Distribution of local Nusselt number at H_D/D_T=1at different Reynolds number for impeller with pitch angle 45°

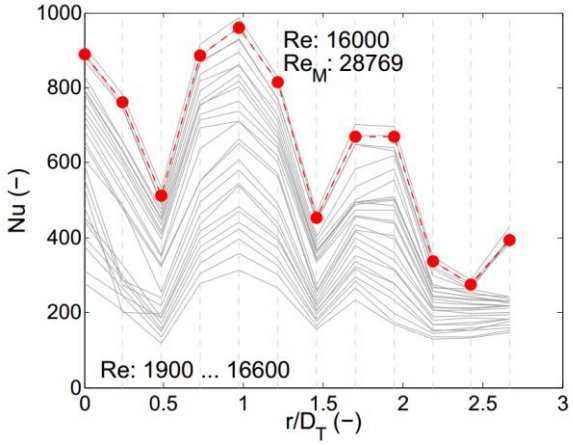

Fig. 9. Distribution of local Nusselt number at H_D/D_T=1at different Reynolds number for impeller with pitch angle 60°.

It can be also seen, that the peaks are not moving in the radial direction in the dependency of Reynolds number. The second peak magnitude increased with Reynolds number, and was higher than the stagnation value in some instances.

The problem with small electrodes lies in the boundary conditions which are not similar to the real case of heat (mass) transfer at the whole surface of the vessel bottom, for example. Therefore the heat transfer coefficient evaluated from equation (2) is larger than the real one because the corresponding width of thermal boundary layer is smaller with small electrodes. Some authors reflect this discrepancy by correction factor p.

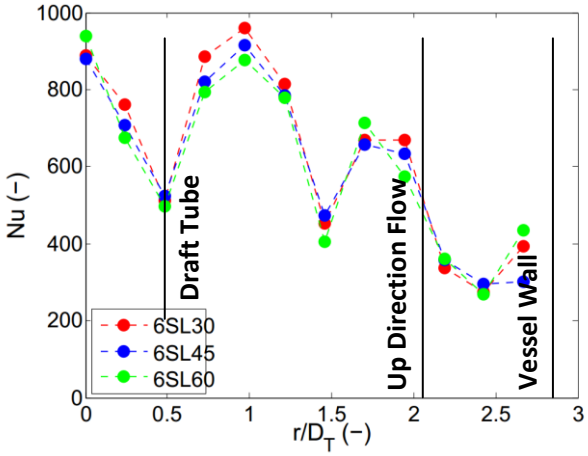

Fig. 10. Distribution of local Nusselt number at H_D/D_T=1 for Re_M =27 239

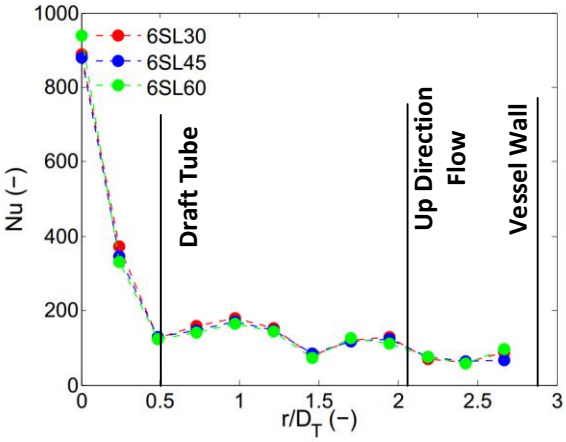

Fig. 11. Distribution of local Nusselt number at H_D/D_T=1 for Re_M =27 239 correctioned by factor p

On the basis of calculated values of Reynolds and Nusselt numbers, were plotted their mutual dependency. From these graphs were determined values of the Reynolds number exponent m

$$Nu = cRe^m \quad (8)$$

The result of these exponent are illustrated in **Fig. 12.**, **Fig. 13.** and **Fig. 14.** It can be seen, that the values of exponents are coincidental.

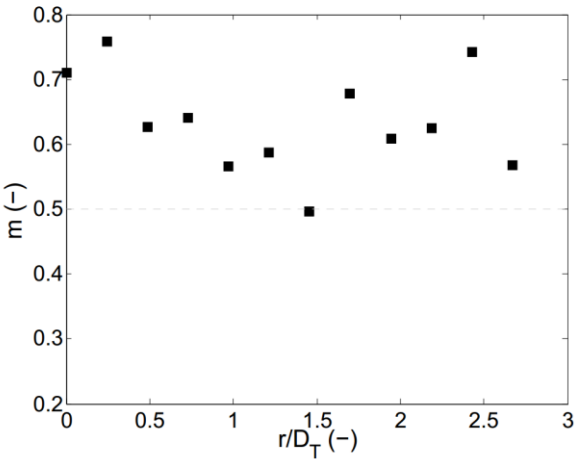

Fig. 12. The dependency of the Reynolds number exponent m on the radial coordinate for impeller with pitch angle 30°

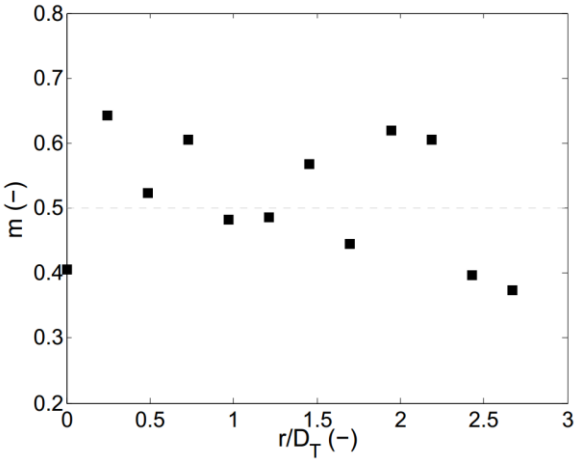

Fig. 13. The dependency of the Reynolds number exponent m on the radial coordinate for impeller with pitch angle 45°

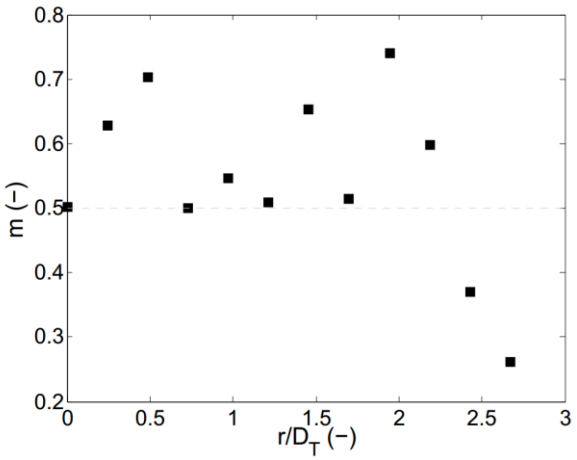

Fig. 14. The dependency of the Reynolds number exponent m on the radial coordinate for impeller with pitch angle 60°

Katti et al. [11] presented experimental results of heat transfer in an unconfined impinging jet and on the basis of these experiments they divided the impinging jet areas into the stagnant region (0≤r/d≤1), transition region (1≤r/d≤2.5) and wall jet region (r/d≥) (see **Fig. 15.).** Values of exponent m in these regions are depicted by thick lines in the figure.

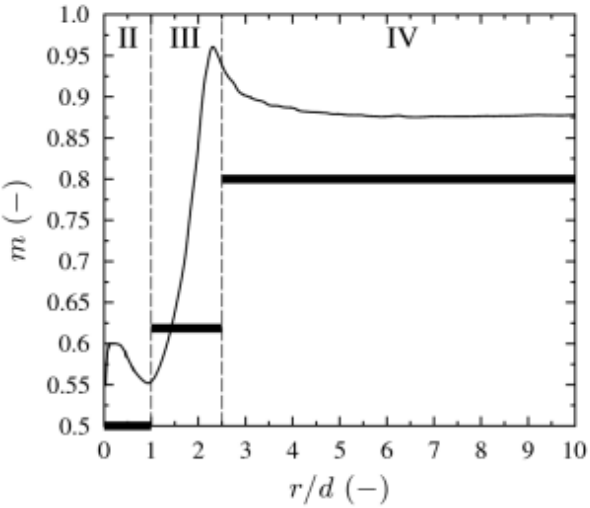

Fig. 15. The dependency of the Reynolds number exponent m on the radial coordinate [11]

From the values of exponent *m* and from **Fig. 15.** it can be deduced, that in our configuration is not developed wall jet along the vessel bottom (region No. IV in **Fig. 1**), because the average value of the exponent is approximately 0.6.

On the basis of calculated values of Nusselt number were also mean values of Nusselt number determined by the formula

$$Nu_{mean} = \frac{2}{R^2}\int_0^R r\, Nu\, dr \qquad (9)$$

In **Fig. 16.**, **Fig. 17.** and **Fig. 18.** can be seen that the mean values of Nusselt number from our measurements are lower than the mean values from literature (green line obtained from equation (1)), but they have the similar slope.

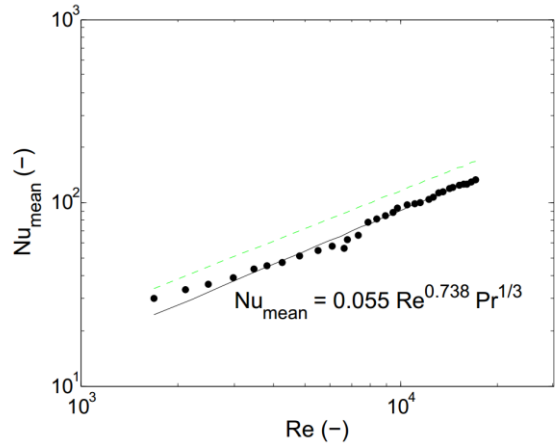

Fig. 16. Relationship between mean value of Nusselt number and Reynolds number for impeller with pitch angle 30°

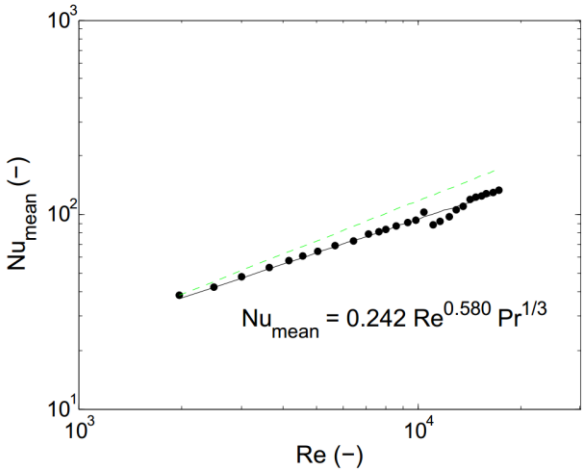

Fig. 17.Relationship between mean value of Nusselt number and Reynolds number for impeller with pitch angle 45°

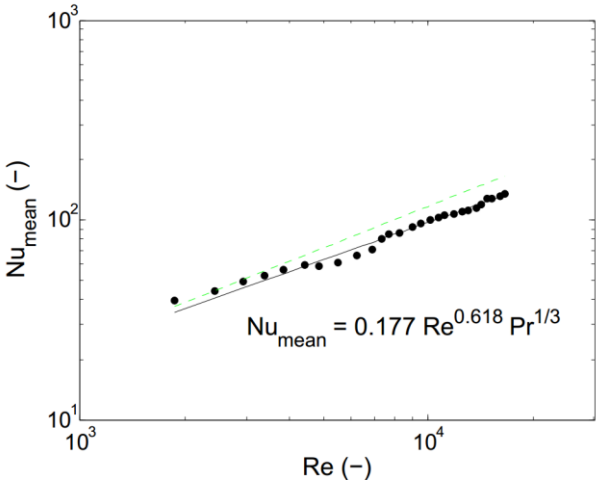

Fig. 18. Relationship between mean value of Nusselt number and Reynolds number for impeller with pitch angle 60°

4. Conclusion

The measurement of the heat transfer on the flat bottom of the vessel agitated by the impeller embedded in the draft using electro-diffusion method was performed. The results were illustrated in form of dependences of the Nusselt number on the Reynolds number (see **Fig. 7.**, **Fig. 8.** and **Fig. 9**) and dependency of the Reynolds number exponent *m* on the ratio r/D_T (see **Fig. 12.**, **Fig. 13.** And **Fig. 14**.).

In the Nu-Re dependences can be seen three peaks. The first one and the second one were expected and they are clearly described by many authors. The third peak, witch one was not expected, is probably caused that fluid flow changes its direction due to presence solid vertical wall.

From comparison of dependences m-r/D_T and the dependency in **Fig. 15.** can be deduced, that in our configuration is not developed wall jet along the vessel bottom (region No.IV in **Fig. 1)**, because the average value of the exponent is approximately 0.6.

The research was carried out only for one configuration of the agitated system; ratio $H_T/D_T=1$. The research will be performed for ratio $H_T/D_T=1/2$ and 1/4 and the results will be publicated.

Symbols

A	Cathode surface area	(m^2)
a	Distance between probes	(m)
b	Baffle width	(m)
C		m
c_A	Molar concentration of the active component in the electrolyte	(mol m^{-3})
c_p	Specific heat capacity	(J kg^{-1} K^{-1})
D	Vessel diameter	(m)
d	Impeller diameter	(m)
D_A	Diffusion coefficient	(m^2 s^{-1})
D_T	Draft tube diameter	(m)
F	Faraday constant	(C mol^{-1})
H	Height of liquid in the vessel	(m)
H_2	Height of impeller above bottom	(m)
H_T	Height of draft tube above bottom	(m)
I	Limiting diffusion current	(A)
k_A	Mass transfer coefficient	(m s^{-1})
l	Baffle length	(m)
L	Draft tube length	(m)
N	Rotational speed of impeller	(s^{-1})
N_{QP}	Dimensionless pumping capacity of impeller	(-)
Pr	Prandtl number (Pr=cpη/λ)	(-)
$\dot{Q}$	Pumping capacity of impeller	(m^3 s^{-1})
R	Vessel radius	(m)
r	Radial coordinate	(m)

Re	Reynolds number	(-)
Re_M	Modified Reynold number ($Re_M=Nd^2/\nu$)	(-)
Sc	Schmidt number ($Sc=D_A/\nu$)	(-)
u	Mean velocity	(m s^{-1})
z	Number of electrons taking part in reaction	(-)
z	Axial coordinate	(m)

α	Heat transfer coefficient	(W m^{-2} K^{-1})
ρ	Density	(kg m^{-3})
ν	Kinematic viscosity	(m^2 s^{-1})
η	Dynamic viscosity	(Pa s)
λ	Thermal conductivity	(W m^{-1} K^{-1})
ν	Kinematic viscosity	(m^2 s^{-1})
m	Reynolds number exponent	(-)

Literatura

[1] MEENA, Hukam Chand, S.A. REODIKAR, Ravish VINZE a S.V. PRABHU. Influence of the shape of the orifice on the local heat transfer distribution between smooth flat surface and impinging incompressible air jet. *Experimental Thermal and Fluid Science*. 2016, **70**, 292-306. DOI: 10.1016/j.expthermflusci.2015.09.018. ISSN 08941777. Dostupné také z: http://linkinghub.elsevier.com/retrieve/pii/S0894177715002551

[2] SCHABEL, Wilhelm a Holger MARTIN. G10 Impinging Jet Flow Heat Transfer. *VDI Heat Atlas* [online]. Berlin, Heidelberg: Springer Berlin Heidelberg, 2010, s. 745 [cit. 2016-04-05]. DOI: 10.1007/978-3-540-77877-6_43. ISBN 978-3-540-77876-9. Dostupné z: http://link.springer.com/10.1007/978-3-540-77877-6_43

[3] FOŘT, Ivan. Flow and turbulence in vessels with axial impeller. UHL, Vincent W. a Joseph B. GRAY. *Mixing: Theory and practice*. 2. Orlando [etc.]: Academic, 1986, s. 133-197. ISBN 0-12-706603-9.

[4] KATTI, Vadiraj V., S. Nagesh YASASWY a S. V. PRABHU. Local heat transfer distribution between smooth flat surface and impinging air jet from a circular nozzle at low Reynolds numbers. *Heat and Mass Transfer* [online]. 2011, **47**(3), 237-244 [cit. 2016-04-13]. DOI: 10.1007/s00231-010-0716-1. ISSN 0947-7411. Dostupné z: http://link.springer.com/10.1007/s00231-010-0716-1

[5] CUDAK, M. a J. KARCZ. Distribution of local heat transfer coefficient values in the wall region of an agitated vessel. *Chemical Papers*. 2008, roč. 62, č. 1, s. 92-99. DOI: 10.2478/s11696-007-0084-6. Dostupné z: http://www.springerlink.com/index/10.2478/s11696-007-0084-6

[6] RIEGER, František, Václav NOVÁK a Tomáš JIROUT. 2005. *Hydromechanické procesy II*. Vyd. 1. Praha: Vydavatelství ČVUT, 167 s. ISBN 80-01-03302-3.

[7] ŠESTÁK, Jiří a Rudolf ŽITNÝ. 2006. *Tepelné pochody II: výměníky tepla, odpařování, sušení, průmyslové pece a elektrický ohřev*. Vyd. 2. V Praze: Nakladatelství ČVUT, 165 s. ISBN 80-010-3475-5.

[8] BROŽ, Jiří, Ivan FOŘT, Reinhard SPERLING, Solomon JAMBERE, Martin HEISER a František RIEGER. 2004. Pumping Capacity of Pitched Blade Impellers in a Tall Vessel with a Draught Tube. *Acta Polytechnica*. Praha: ČVUT, **44**(4): 48-53. ISSN 1805-2363.

[9] RIEGER, František, Václav NOVÁK a Tomáš JIROUT. 2005. *Hydromechanické procesy I*. Vyd. 1. Praha: Vydavatelství ČVUT, 209 s. ISBN 80-01-03283-2.

[10] CFD simulace proudění v míchacím zařízení s usměrňovačem toku – *Vlček, P. - Jirout, T.*, In: Sborník konference CHISA 2015. Praha: Česká společnos t chemického inženýrství, 2015,

[11] KATTI, Vadiraj a S.V. PRABHU. Experimental study and theoretical analysis of local heat transfer distribution between smooth flat surface and impinging air jet from a circular straight pipe nozzle. *International Journal of Heat and Mass Transfer*. 2008, **51**(17-18), 4480-4495. DOI: 10.1016/j.ijheatmasstransfer.2007.12.024. ISSN 00179310. Dostupné také z: http://linkinghub.elsevier.com/retrieve/pii/S0017931008000768

[12] BOVO, Mirko. *On the numerical modelling of impinging jets heat transfer*. Gothenburg, 2011. Thesis. Chalmers university of technology, Depatment of Applied mechanics.

Acknowledgement

This work was supported by the Grand Agency of the Czech Technical University in Prague, grant No. SGS16/149/OHK2/2T/12